Observation of heat flow at transition temperature in $La_{1-x}Ca_xMnO_{3+\delta}$ Oxides

Y. B. Zhang, S. Li,[a] and C. Q. Sun
School of Materials Engineering, Nanyang Technological University, Singapore 639798, Singapore

W. Gao
School of Engineering, The University of Auckland, Auckland 1020, New Zealand

S. X. Dou
Institute for Superconducting and Electronic Materials, University of Wollongong, Wollongong NSW 2522, Australia

P. Hing
School of Materials Engineering, Nanyang Technological University, Singapore 639798, Singapore

(Received 8 February 2001; accepted for publication 1 August 2001)

Heat-flow changes of $La_{1-x}Ca_xMnO_{3+\delta}$ (x=0.25, 0.33, and 0.375) magnetoresistive oxides at their Curie temperatures have been detected using differential scanning calorimetry in the temperature range from 173 to 293 K. However, the transition does not occur in the samples of x=0.125 and 0.5. It was found that the heat flow reflected the transition behavior and the enthalpy change of the transition decreased as the transition temperature increased. These results indicate that the $La_{1-x}Ca_xMnO_{3+\delta}$ oxides (x=0.25, 0.33, and 0.375) undergo an endothermic phase transition from a low-temperature ferromagnetic metal to a high-temperature paramagnetic insulator. It is assumed that the transition is strongly associated with a local structure change, which is correlated with the metal–insulator transition. © *2001 American Institute of Physics.* [DOI: 10.1063/1.1406551]

INTRODUCTION

The electron transport behavior of mixed-valence $La_{1-x}A_xMnO_{3+\delta}$ (A=Ca, Sr, and Ba) oxides has attracted attention because of their colossal magnetoresistance property.[1–7] It is known that the maximum magnetoresistance occurs around the temperature of a transition from paramagnetic insulating state to ferromagnetic metallic state. Since the double exchange mechanism[8–10] could not sufficiently explain the colossal magnetoresistivity around the transition temperature (T_c),[11] the lattice polaron theory in the paramagnetic state has been used to describe the magnetoresistance behavior recently.[12,13] The changes in thermal parameters, such as thermopower Q, and isotropic Debye–Waller factor $\langle u^2 \rangle$, associated with the ferromagnetic–paramagnetic and metal–insulator transition, have been intensively studied for understanding the mechanism of lattice polaron effects on the transition behavior.[14,15] It has been reported that the $La_{1-x}Ca_xMnO_{3+\delta}$ oxides with x=0.2–0.5 doping level undergo a transition from ferromagnetic metal to paramagnetic insulator (FMM–PMI) while the $La_{0.875}Ca_{0.125}MnO_{3+\delta}$ oxide transits from a ferromagnetic insulator to a paramagnetic insulator (FMI–PMI), in the heating process.[16] However, the mechanism of Ca doping level effect on the polaron behavior in the transition of $La_{1-x}Ca_xMnO_{3+\delta}$ oxides has not been clearly understood yet and no report related to heat flow in the $La_{1-x}A_xMnO_{3+\delta}$ manganite system has been seen. In the present work, we report on the observations of the heat flow of $La_{1-x}Ca_xMnO_{3+\delta}$ (x=0.125, 0.25, 0.33, 0.375, and 0.5) oxides and explore the possible mechanism of the phase transition based on thermodynamic theories. The ferromagnetic to paramagnetic transition is the second order transition in thermodynamics. However, the heat flow transition in the samples of $La_{1-x}Ca_xMnO_{3+\delta}$ (x=0.25, 0.33, and 0.375) oxides reflects a local structure transition of first order together with the second order magnetic transition.

EXPERIMENT

Ceramic samples of $La_{1-x}Ca_xMnO_{3+\delta}$ (x=0.125, 0.25, 0.33, 0.375, and 0.5) were synthesized by the solid-state reaction method. The La_2O_3 (99.99%), $CaCO_3$ (>99%), and MnO_2 (99.99%) powders were mixed with a nominal stoichiometry of La:Ca:Mn=$(1-x):x:1$, ground to a fine mixture. The La_2O_3 powder was dried at 1173 K for 2 h to avoid the hygroscopicity of the La_2O_3 compound before weighting. The powder mixture was calcined at 1073 K for 24 h to decompose calcium carbonate to calcium oxide. The decomposed powder mixture was ground and pressed into pellets and subsequently sintered at 1573 K for 60 h in air to form $La_{1-x}Ca_xMnO_{3+\delta}$ oxides. The sintered oxides were then ground and pressed into pellets again and finally sintered at 1573 K for 60 h in air atmosphere. It is assumed that the oxygen stoichiometry in the perovskite oxides is dependent on the oxygen-loading rate, which is dominated by the cooling process. In the present work, the samples of $La_{1-x}Ca_xMnO_{3+\delta}$ oxides were cooled with the identical rate and the oxygen stoichiometry can be considered to be similar

[a]Author to whom correspondence should be addressed; Electronic mail: assxli@ntu.edu.sg

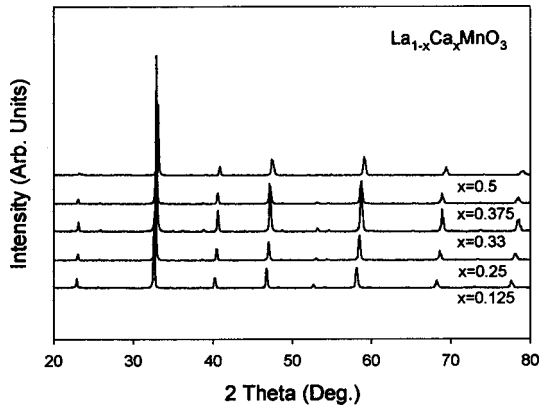

FIG. 1. X-ray diffraction patterns of $La_{1-x}Ca_xMnO_{3+\delta}$ oxides.

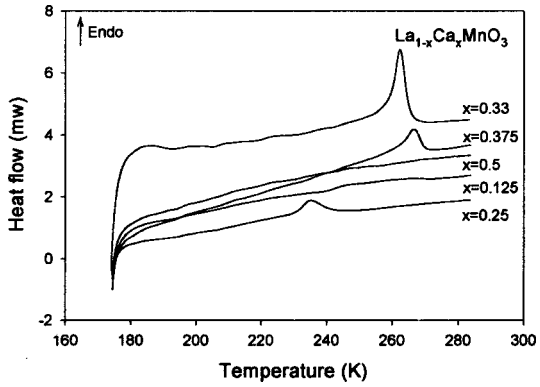

FIG. 3. Raw heat flow vs temperature for $La_{1-x}Ca_xMnO_{3+\delta}$ oxides in the heating process.

in these samples. It was reported that the deviation of the oxygen stoichiometry of the $La_{1-x}Ca_xMnO_{3+\delta}$ oxides prepared by the aforementioned technique is less than 1% from the $La_{1-x}Ca_xMnO_3$ oxide ($|\delta|<0.01$).[16] To analyze the effect of the dopant level on the lattice structure and transition behavior, the as-prepared materials were characterized by x-ray diffraction (XRD). The heat flow was measured with differential scanning calorimetry (DSC) (SETARAM, DSC 131) in the temperature range from 173 to 293 K with the scanning rate of 5 K/min.

RESULTS AND DISCUSSION

The XRD spectra of $La_{1-x}Ca_xMnO_{3+\delta}$ ($x=0.125$, 0.25, 0.33, 0.375, and 0.5) oxides in Fig. 1 show that all materials had pure orthorhombic (*Pbnm*) perovskite-like structures. However, the spectra exhibited the shift of diffraction peaks, especially at high diffraction angles. The relative intensities of the peaks were also different in these spectra, as shown in the figure. The lattice parameters *a*, *b*, *c* and unit-cell volume versus Ca doping level are plotted in Fig. 2. The experimental results are in good agreement with the results obtained by others in $La_{0.75}Ca_{0.25}MnO_3$ and $La_{0.5}Ca_{0.5}MnO_3$.[17] It was found that the lattice parameters and unit-cell volume decreased with the Ca doping level increase and there were plateaus appearing in the curves between $x=0.33$ and $x=0.375$. This effect was not only related to the substitution of Ca^{2+} ions for the larger La^{3+} ions, but was also due to the conversion of Mn^{3+} into Mn^{4+} in *x* stoichiometry. In fact, the Mn–O–Mn bond length and angle dominate the lattice parameters.[18] Therefore, it can be inferred that the Mn–O–Mn bond length and angle are also strongly affected by the Ca doping level, thus resulting in different local lattice distortion.

Figure 3 presents the raw DSC spectra of $La_{1-x}Ca_xMnO_{3+\delta}$ ($x=0.125$, 0.25, 0.33, 0.375, and 0.5) oxides in the heating process. It indicates that the first order endothermic phase transition only occurred in the samples of $x=0.25$, 0.33, and 0.375, while there was not such a transition in the samples of $x=0.125$ and 0.5. Based on the transition diagram of $La_{1-x}Ca_xMnO_{3+\delta}$ oxides,[16] the endothermic phase transition could be considered to reflect the FMM-PMI transition. The change of Gibbs free energy in this transition can be expressed as $\Delta G=\Delta H-T\Delta S$. When the transition occurs, the system reaches an equilibrium state and $\Delta G=0$. Therefore, $\Delta S=\Delta H/T$. The endothermic phase transition($\Delta H>0$) implies that the disorder degree of the system increased as the transition took place. It was reported that, in the FMM to PMI transition, the bond lengths of Mn–O are uniformly distributed below T_c, while the bond lengths are different, thus presenting a disorder state above T_c.[13] When the uniform Mn–O bond lengths were modified to different lengths, the undistorted Mn–O octahedra at lower temperature transformed to the distorted octahedra at higher temperature, thus the system was converted from the order state to the disorder state. This phenomenon implies that the heat flow peak is associated with the local lattice structure change.

It was proposed that the local lattice structure change originated from the delocalization and transportation of charge carriers (holes) in the oxides as a result of bond relaxation below T_c.[13] In the FMM state, the holes were delo-

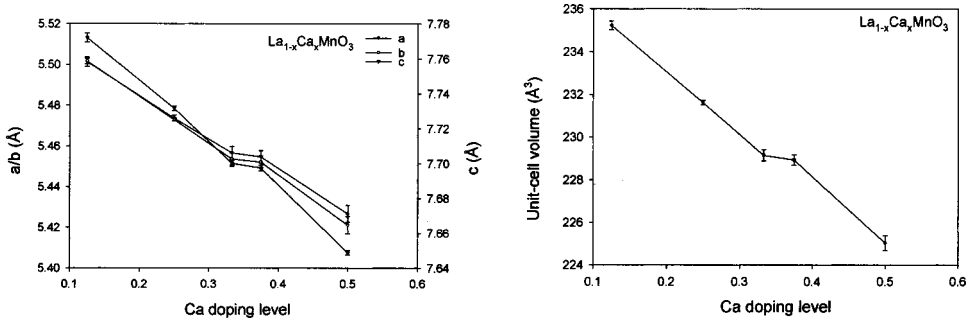

FIG. 2. Lattice parameters and unit-cell volume vs Ca doping level.

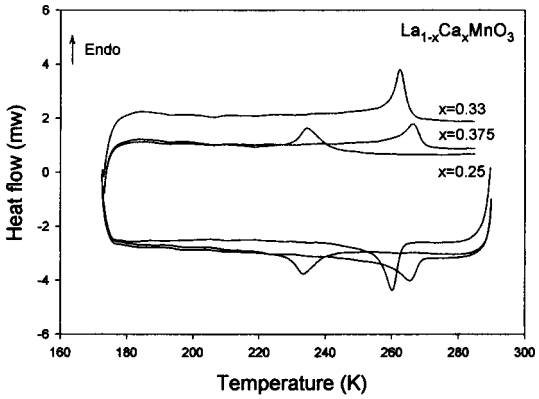

FIG. 4. Heat flow vs temperature for $La_{1-x}Ca_xMnO_{3+\delta}$ (x=0.25, 0.33, and 0.375) oxides in the cooling, isothermal, and heating process.

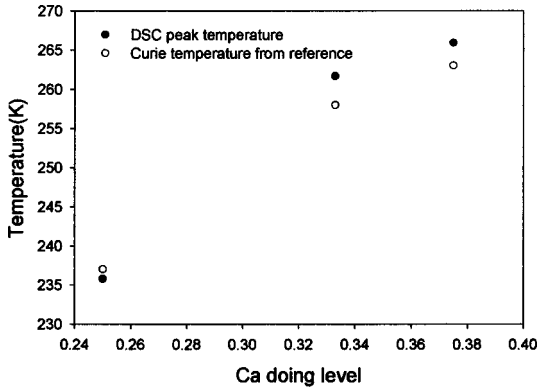

FIG. 5. DSC peak temperature for the endothermic transition of $La_{1-x}Ca_xMnO_{3+\delta}$ (x=0.25, 0.33, and 0.375) oxides and their Curie temperature.

calized and the distortion of the Mn–O octahedra was uniformly averaged at the temperature below T_c. However, the extent of delocalization was strongly affected by the interaction between lattice and polarons, which are localized conduction band electrons. In this case, the Ca doping level may dominate the interaction because of the difference in hole concentration. The effect of doping a small amount of Ca, such as x=0.125, on the delocalization of the small amount of holes was too weak to affect the delocalization of the holes and restructure the Mn–O bond length from the disorder state to the order state at the lower temperature. It resulted that no transition took place in the measurement temperature range.

On the other hand, it is assumed that the interaction between lattice and polarons is mainly attributed to the synthesized effects, such as the hole concentration and the difference of ionic radii between La^{3+} and Ca^{2+}, and also Mn^{3+} and Mn^{4+}. These effects offset each other. Once the Ca doping level reached x=0.5, the cancellation of these effects may strongly minimize the interaction. It suggests that the delocalization of the holes did not take place in the cooling process, thus resulting in $La_{0.5}Ca_{0.5}MnO_{3+\delta}$ oxide having a similar transition behavior like $La_{0.875}Ca_{0.125}MnO_{3+\delta}$ oxide, i.e., no transition in the measurement temperature range.

The heat flow versus temperature for $La_{1-x}Ca_xMnO_{3+\delta}$ (x=0.25, 0.33, and 0.375) oxides in the cooling, isothermal, and heating process is plotted in the Fig. 4. The heat flow was determined by the baseline subtraction from the raw heat flow. For the heat flow spectrum of each sample, the apparent transition widths in temperature were the same for heating and cooling with the identical scanning rate of 5 K/min. The temperature hysteresis for endothermic and exothermic peaks in the samples of x=0.25, 0.33, and 0.375 was 1.1, 2.2, and 1.0 K, respectively. It was reported that the lattice parameters and unit-cell volume as a function of temperature in $La_{0.75}Ca_{0.25}MnO_3$ and $La_{0.65}Ca_{0.35}MnO_3$ demonstrated the presence of a lattice contraction below their respective T_c, with an abrupt decrease of all lattice parameters and a volume discontinuity.[15,17] The results above evidence that the transitions are thermodynamically of first order. However, the largest temperature hysteresis occurred in the sample of x=0.33, which has the largest magnetoresistance (MR) property. It is not clear whether the largest temperature hysteresis can reflect the mechanism of the largest MR property occurring in $La_{0.67}Ca_{0.33}MnO_{3+\delta}$ oxide.

The transition temperature (the temperature of the peak in heat flow spectrum) against Ca doping level from x=0.25 to x=0.375 for the endothermic phase transition is plotted in Fig. 5. Their Curie temperature T_c from Ref. 16 is also plotted for comparison. It indicates that the transition temperature of the oxides increased with the Ca doping level increasing and the Ca doping level in x=0.375 showed the highest transition temperature. It is proposed that the lattice distortion of $La_{1-x}Ca_xMnO_{3+\delta}$ oxides may be affected by two factors. One is the percentage of the large Jahn–Teller distortion ion, Mn^{3+} (d^4), at manganese ion sites. The lattice distortion decreases with the number of Mn^{3+} ions decreasing. The other is concentration of doped Ca^{2+} ions substituting for La^{3+} ions. The lattice distortion increases with increasing the concentration of Ca^{2+} since the radius of Ca^{2+} is smaller than that of La^{3+}. However, the concentration increase of Ca^{2+} results in the concentration decrease of Mn^{3+}. This suggests that there is an optimal concentration of Ca^{2+}, which minimizes the lattice distortion in the $La_{1-x}Ca_xMnO_{3+\delta}$ oxides. This may be the reason for the existence of the aforementioned plateaus in the curves of lattice parameters and unit-cell volume versus Ca doping level. It was reported that high lattice distortion results in low T_c because of the narrowing of the $e_g(\mathrm{Mn})-2p_\sigma(\mathrm{O})-e_g(\mathrm{Mn})$ conduction bandwidth.[19] Based on the analysis above and Fig. 5, it can be inferred that the peak temperature of phase transitions reflected T_c. Therefore, the transition temperature increased with the lattice distortion decrease and the $La_{0.625}Ca_{0.375}MnO_{3+\delta}$ oxide showed the highest T_c due to the lowest lattice distortion in our sample series.

Figure 6 presents the enthalpy change in the FMM–PMI phase transition of $La_{1-x}Ca_xMnO_{3+\delta}$ (x=0.25, 0.33, and 0.375) oxides. Since heat capacity (dH/dT) can be computed from heat flow (dH/dt) and scanning rate (dT/dt), the heat capacity can be integrated to obtain the area of the endothermic peak in the heat flow spectrum with a certain scanning rate. The integrated area depicts the enthalpy change in the transition. A series of experiments were con-

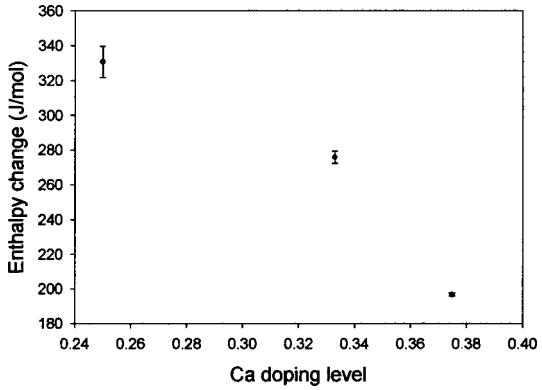

FIG. 6. Enthalpy change in the FMM–PMI phase transition of $La_{1-x}Ca_xMnO_{3+\delta}$ ($x=0.25$, 0.33, and 0.375) oxides.

ducted to investigate the effect of the temperature-scanning rate on the enthalpy change[20] and the results show that the effect is marginal since the difference in superheating temperature due to different scanning rate in the heating process can be negligible. Therefore, the enthalpy change obtained with the scanning rate of 5 K/min can represent the real enthalpy change in the FMM–PMI transition at an equilibrium state. Figure 6 shows that the enthalpy change in the transitions decreased with the Ca doping level increase. It implies that the enthalpy change is strongly related to the degree of lattice distortion in the $La_{1-x}Ca_xMnO_{3+\delta}$ oxides ($x=0.25$, 0.33, and 0.375). The gain of total entropy in the FMM–PMI transition can be calculated according to $\Delta S = \Delta H/T$. It was found that the total entropy change in the transition was relatively small compared to the gain of spin entropy that results from the spin disordering. For example, the gain of spin entropy for $La_{0.67}Ca_{0.33}MnO_3$ is approximately 6.7 (1/2R ln5, R: Gas constant) J/(mol K)[21] while the total entropy change is 1.1 J/(mol K). It is assumed that the difference is due to a loss of lattice entropy from electron localization in the FMM–PMI transition. It may be deduced that the higher distorted material has less loss of lattice entropy from electron localization, resulting in more thermal energy the system absorbed for the transition. Hence, the enthalpy change increased with the local lattice distortion increase. Moreover, it can be summarized that, in the $La_{1-x}Ca_xMnO_{3+\delta}$ ($x=0.25$, 0.33, and 0.375) oxides, the enthalpy change in the transition increases as the transition temperature decreases because of the increasing lattice distortion.

CONCLUSION

In conclusion, the endothermic peaks of the $La_{1-x}A_xMnO_{3+\delta}$ ($x=0.25$, 0.33, and 0.375) oxides in FMM–PMI transition reflect that the transition is the first order phase transition associated with a local structure transition. The metal–insulator transition in the $La_{1-x}A_xMnO_{3+\delta}$ oxides may originate from the formation of polarons in the paramagnetic insulating state. The enthalpy change in the transition is strongly affected by the local lattice structure change, which is related to lattice distortion. This phenomenon does not occur at the lower or higher Ca doping level, where only a magnetic transition without local lattice structure change takes place. No local structure transition in $La_{0.88}Ca_{0.12}MnO_3$ can be detected while a local structure change in $La_{0.75}Ca_{0.25}MnO_3$ was found using pair-distribution function analysis of neutron powder-diffraction data.[13] Further experiments will be conducted to determine the hypothesis, which may reflect the information about local structure around Curie temperature, for the materials with other Ca doping levels.

[1] R. von Helmolt, J. Wecker, B. Holzapfel, L. Schultz, and K. Samwer, Phys. Rev. Lett. **71**, 2331 (1993).
[2] R. Mahendiran, A. K. Raychaudhuri, A. Chainani, D. D. Sarma, and S. B. Roy, Appl. Phys. Lett. **66**, 233 (1995).
[3] S. Jin, T. H. Tiefel, M. McCormack, R. A. Fastnacht, R. Ramesh, and J. H. Chen, Science **264**, 413 (1994).
[4] M. McCormack, S. Jin, T. H. Tiefel, R. M. Fleming, Julia M. Phillips and R. Ramesh, Appl. Phys. Lett. **64**, 3045 (1994).
[5] S. Jin, M. McCormack, T. H. Tiefel, and R. Ramesh, J. Appl. Phys. **76**, 6929 (1994).
[6] S. Jin, T. H. Tiefel, M. McCormack, H. M. O'Bryan, L. H. Chen, R. Ramesh, and D. Schurig, Appl. Phys. Lett. **67**, 557 (1995).
[7] S. Jin, H. M. O'Bryan, T. H. Tiefel, M. McCormack, and W. W. Rhodes, Appl. Phys. Lett. **66**, 382 (1995).
[8] C. Zener, Phys. Rev. **81**, 440 (1951).
[9] C. Zener, Phys. Rev. **82**, 403 (1951).
[10] P. G. de Gennes, Phys. Rev. **118**, 141 (1960).
[11] A. J. Millis, P. B. Littlewood, and B. I. Shraiman, Phys. Rev. Lett. **74**, 5144 (1995).
[12] H. Röder, J. Zhang, and A. R. Bishop, Phys. Rev. Lett. **76**, 1356 (1996).
[13] S. J. L. Billinge, R. G. Difrancesco, G. H. Kwei, J. J. Neumeier, and J. D. Thompson, Phys. Rev. Lett. **77**, 715 (1996).
[14] J. Fontcuberta, A. Seffar, X. Granados, J. L. Garcia-Munoz, X. Obradors, and S. Pinol, Appl. Phys. Lett. **68**, 2288 (1996).
[15] P. Dai, J. D. Zhang, H. A. Mook, F. Foong, S.-H. Liou, P. A. Dowben, and E. W. Plummer, Solid State Commun. **100**, 865 (1996).
[16] P. Schiffer, A. P. Ramirez, W. Bao, and S-W. Cheong, Phys. Rev. Lett. **75**, 3336 (1995).
[17] P. G. Radaelli, D. E. Cox, M. Marezio, S-W. Cheong, P. E. Schiffer, and A. P. Ramirez, Phys. Rev. Lett. **75**, 4488 (1995).
[18] J. Blasco, J. Garcia, J. M. de Teresa, M. R. Ibarra, P. A. Algarabel, and C. Marquina, J. Phys.: Condens. Matter **8**, 7427 (1996).
[19] J. L. Garcia-Munoz, J. Fontcuberta, M. Suaaidi, and X. Obradors, J. Phys.: Condens. Matter **8**, 787 (1996).
[20] Y. B. Zhang, S. Li, P. Hing, C. Q. Sun, W. Gao, and S. X. Dou, Solid State Commun. **120**, 107 (2001).
[21] A. P. Ramirez, P. E. Schiffer, S-W. Cheong, C. H. Chen, W. Bao, T. T. M. Palstra, P. L. Gammel, D. J. Bishop, and B. Zegarski, Phys. Rev. Lett. **76**, 3188 (1996).